

Citation: M. J. Goldsworthy, M. N. Macrossan and M. M. Abdel-jawad (2007) Nonequilibrium reaction rates in the macroscopic chemistry method for direct simulation Monte Carlo calculations, *Physics of Fluids* 19: 066101. doi: 10.1063/1.2742747

NON-EQUILIBRIUM REACTION RATES IN THE MACROSCOPIC CHEMISTRY METHOD FOR DSMC CALCULATIONS

M.J. GOLDSWORTHY¹, M.N. MACROSSAN¹ & M.M ABDEL-JAWAD²

March 19, 2007

The Direct Simulation Monte Carlo (DSMC) method is used to simulate the flow of rarefied gases. In the Macroscopic Chemistry Method (MCM) for DSMC, chemical reaction rates calculated from local macroscopic flow properties are enforced in each cell. Unlike the standard total collision energy (TCE) chemistry model for DSMC, the new method is not restricted to an Arrhenius form of the reaction rate coefficient, nor is it restricted to a collision cross-section which yields a simple power-law viscosity. For reaction rates of interest in aerospace applications, chemically reacting collisions are generally infrequent events and, as such, local equilibrium conditions are established before a significant number of chemical reactions occur. Hence, the reaction rates which have been used in MCM have been calculated from the reaction rate data which are expected to be correct only for conditions of thermal equilibrium. Here we consider artificially high reaction rates so that the fraction of reacting collisions is not small and propose a simple method of estimating the rates of chemical reactions which can be used in the Macroscopic Chemistry Method in both equilibrium and non-equilibrium conditions.

Two tests are presented: (1) The dissociation rates under conditions of thermal non-equilibrium are determined from a zero-dimensional Monte-Carlo sampling procedure which simulates ‘intra-modal’ non-equilibrium; that is, equilibrium distributions in each of the translational, rotational and vibrational modes but with different temperatures for each mode; (2) The 2-D hypersonic flow of molecular oxygen over a vertical plate at Mach 30 is calculated. In both cases the new method produces results in close agreement with those given by the standard TCE model in the same highly nonequilibrium conditions. We conclude that the general method of estimating the non-equilibrium reaction rate is a simple means by which information contained within non-equilibrium distribution functions predicted by the DSMC method can be included in the Macroscopic Chemistry Method.

¹ Centre for Hypersonics, The University of Queensland, Brisbane, 4067, Australia

² ARC Centre for Functional Nanomaterials, The University of Queensland, Brisbane, 4067, Australia

I. MODELLING OF CHEMICAL REACTIONS IN DSMC

Inclusion of chemical reactions in the DSMC method has been considered by many authors and recently summarized by Boyd¹. Traditionally, these ‘conventional’ models are collision based; when two particles are chosen to collide, a reaction probability is computed if there is sufficient energy for the particles to reach the product state. Since there is limited information on state-specific reaction probabilities for the reactions of interest in aerodynamics, probability functions have generally been developed on a phenomenological basis and the models are calibrated to reproduce experimental reaction rates under conditions of thermal equilibrium. Validation of these models under conditions of thermal non-equilibrium has, with recent exception, generally consisted of comparisons with other DSMC simulations, rather than with experimental results²⁻⁵.

The standard chemistry method for DSMC is the total collision energy (TCE) method of Bird⁶. The TCE method is formulated for collision probabilities matching the variable hard sphere (VHS) total collision cross-section, and for equilibrium chemical reaction rate coefficients in the Arrhenius form. A different collision cross-section, which might be required to yield a certain viscosity $\mu = \mu(T)$, or a multi-temperature reaction rate model cannot be used. In response to these difficulties, the macroscopic chemistry method (MCM) was proposed by Lilley and Macrossan⁷. In this method, chemical reactions are not processed on a collision pair basis. Instead a reaction rate is calculated from the state information in each cell to determine the total number of ‘reaction events’ required at any time step. The number of molecules or atoms in the cell is then adjusted to conform with the required number of reaction events. The reaction rate in the MCM may be derived from *any* experimental or theoretical source, and it may be based on *any* macroscopic parameters.

In previous applications of MCM⁷⁻¹⁰ the reaction rates have been calculated (1) from the kinetic temperature in an Arrhenius rate equation, (2) from the density-dependent reaction rates given by Gupta *et al.*¹¹, and (3) from the two-temperature model of Park¹². In the first two examples, the reaction rate was taken as the value expected for conditions of thermal equilibrium. It was argued that chemically reacting collisions are infrequent events and, as such, local equilibrium conditions are established before a significant number of chemical reactions occur. If the fraction of collisions which result in a chemical reaction is not small, then it would be necessary to account for the non-equilibrium distribution of energy in collisions.

In order to capture some of the information contained within the non-equilibrium distribution functions predicted by the DSMC method and which is not included in thermally averaged experimental rate data, we propose a simple reaction rate adjustment. The adjustment is such that if the rate of sufficiently energetic collisions is found to differ from the theoretically expected rate at the local equilibrium condition, the reaction rate is modified in proportion to the difference.

II. CORRECTION FOR NON-EQUILIBIRUM RATES

The problems for which the DSMC method is commonly applied involve predominately bimolecular chemical reactions. These elementary reactions require two-body collisions, a common example being the dissociation of a molecule through collisions with a second molecule or atom. If the reaction is given by: $A + B \rightarrow products$, then the rate of depletion of a reactant species can be expressed as:

$$\frac{dN_A}{dt} = k_f N_A \cdot N_B \quad [1]$$

Here N_i is the number density of species 'i', and k_f is a rate coefficient with units of a reaction volume per unit time. Following Vincenti and Kruger¹³, the rate of reactant depletion can be expressed in the form of:

$$\frac{dN_A}{dt} = Z_{AB} \cdot F \cdot S \quad [2]$$

Here Z is the bimolecular collision rate for the species of interest, F is the fraction of all such collision pairs which have energy above a threshold value and S is the fraction of collision pairs satisfying the energy criteria which actually react (the steric factor). This expression is convenient in that it is physically intuitive and can be used to derive an approximate theoretical expression for the reaction rate. The rate coefficient for the reaction can thus be expressed as:

$$k_f = \frac{Z_{AB}}{N_A N_B} \cdot F \cdot S = Z_c \cdot F \cdot S \quad [3]$$

Here Z_c is the collision constant, analogous to the rate constant, with units of collision volume per unit time. Each of the terms on the RHS may be interpreted as averaged quantities where the averaging is over an ensemble of collisions.

Here we assume that the steric factor under thermal non-equilibrium conditions is equal to the steric factor at a nearby equilibrium condition. Hence, we propose that the reaction rate in conditions of thermal equilibrium or non-equilibrium may be approximated as

$$k_f = k_f^* \cdot \frac{Z_{AB}}{Z_{AB}^*} \cdot \frac{F}{F^*} \quad [4]$$

In this equation (*) denotes equilibrium conditions and the equation reduces to $k_f = k_f^*$ at equilibrium.

The actual non-equilibrium collision rate Z_{AB} , and non-equilibrium fraction of colliding particle pairs with energy greater than the threshold F , are monitored during the collision selection procedure. We could equally well consider the ratio of the *rate* of non-equilibrium to equilibrium high energy collisions. If, during the collision calculations for any cell, there are fewer high energy collisions than expected for equilibrium conditions, then the chemical reaction rate k_f given by Eq. 4 is proportionally less than k_f^* .

III. IMPLEMENTATION

The above rate correction which accounts for the actual collision rate and high energy portions of the distribution may be implemented in the MCM DSMC routine with little computational cost. The implementation discussed here refers to a reaction rate model without biasing for a particular energy mode. Although such a model is known to be insufficient, given for example the influence of coupled vibrational motion and dissociation, our purpose is to demonstrate the general procedure for correcting equilibrium rates for thermal non-equilibrium conditions. Corrections including the preferential treatment of specific energy modes are a topic for later investigation.

At the start of the simulation, reaction rates are computed using the equilibrium expressions. As the collisions are computed, the total number of collisions and the number with energy from the specified degrees of freedom in excess of the threshold energy are counted. The expected equilibrium collision rate and high energy fraction are computed from the time-averaged macroscopic cell parameters.

Although the method may be applied generally to *any* DSMC collision routine, expressions for the variable hard sphere (VHS) model⁶ with continuously distributed internal energy modes are given here:

$$Z_c^* = \frac{2\sigma_{ref} g_{ref}^{2\nu} \Gamma(2-\nu)}{\sqrt{\pi}} \left(\frac{\tilde{m}}{2kT} \right)^{\nu-0.5} \quad F^* = \frac{\Gamma(2-\nu + \bar{\zeta}_{int}, E_o/kT)}{\Gamma(2-\nu + \bar{\zeta}_{int})} \quad [5]$$

Here σ_{ref} and g_{ref} are reference values of the collision cross-section and relative speed, $(\nu + 0.5)$ is the temperature exponent in the power law viscosity relation, \tilde{m} is the reduced mass, $\bar{\zeta}_{int}$ is the number of internal degrees of freedom, k is Boltzmann's constant and E_o is the threshold energy.

The rate correction compares the actual collision rate and high energy fraction with that expected at a 'nearby' equilibrium condition. The fact that the collision rate is proportional to the translational temperature implies that the translational temperature be used to evaluate the equilibrium condition. On the other hand, since the high energy fraction F^* is proportional to all the energy available in collisions, it may well be more appropriate to evaluate the equilibrium values of Z_c^* and F^* using an overall temperature defined by:

$$T_{ov} = \frac{3T_t + \bar{\zeta}_r T_r + \bar{\zeta}_v T_v}{3 + \bar{\zeta}_r + \bar{\zeta}_v} \quad [6]$$

However, since the actual collision rate and high energy fraction are always accounted for by the method, the differences due to the temperature chosen arise only in the form of the departure of the actual steric factor from the equilibrium one. In this study, T_{ov} is used to evaluate the reaction rate. The computational time for evaluation of Z_c^* and F^* is negligible since they are evaluated only when the macroscopic cell parameters are updated using the accumulated sample collected in each cell.

IV. RESULTS

Since we are considering the case where there is no biasing for a particular energy mode, we compare the non-equilibrium MCM rates with those predicted by the TCE model. The correct non-equilibrium chemical reaction rates are not known, but the proposed rate calculation is inspired by the physical modelling of the TCE method. Agreement of our model with the TCE model does not indicate that MCM yields correct reaction rates, but only that it can be used to obtain plausible non-equilibrium rates.

Wadsworth and Wyson⁵ argue that comparisons of the non-equilibrium rate coefficients are a poor test of DSMC chemistry models. The temperature dependence of the rate is primarily due to the exponential term which accounts for the threshold energy and the chemistry models essentially differ only in their interpretation of the steric factor. They say that it is more accurate to compare the energy distributions of those pairs selected for reaction. However, such detailed comparisons are neither necessary nor informative in this case. The reason is that in the MCM, the selection procedure for reactant particles is completely decoupled from the number of reaction events which occur; it is possible in MCM to adjust independently the number of reaction events and the energy distributions of post reaction particles through the use of different energy disposal models. Since we consider here only a rate correction, comparisons of the non-equilibrium rate coefficients predicted by the MCM are sufficient to investigate the ability of the method to resolve chemical reaction rates in regions of thermal non-equilibrium.

We consider two methods of comparing reaction rates in thermal non-equilibrium. A zero-dimensional Monte-Carlo collision sampling program is used to investigate a special case of non-equilibrium which we refer to as ‘intra-modal’ non-equilibrium. By this, we mean that even though the kinetic temperatures of each energy mode are different, the energy within each mode conforms to the Boltzmann distribution. The rate correction is aimed at accounting for the different distributions of energy in collision pairs owing to a non-equilibrium partitioning of energy between the modes. Although the total collision energy is constant and there is no preference for energy in a particular mode, different reaction rates can arise due to varying collision rates, different amounts of energy absorbed in the motion of the centre of mass of collision pairs and the varying quantity of energy stored in the vibrational mode.

In the second method, comparisons are made based on a highly non-equilibrium 2D flow simulation. This is the most general comparison since chemical reactions may arise from regions which contain any realistic energy distributions.

A. MONTE CARLO SAMPLING

A Monte-Carlo sampling procedure has been used to sample translational, rotational and vibrational energy for potential collision pairs from the actual equilibrium distribution functions where each distribution is considered at a different temperature. The simulation is zero-dimensional in that molecules are not moved. Potential collision pairs are selected using the acceptance-rejection NTC collision procedure⁶ with the VHS collision model. The maximum value of the product of the collision cross-section and relative speed is set as a constant, large value. Although computationally inefficient, this method allowed for varying temperatures in the individual translational components. The TCE reaction probability is then computed and the number of successful reaction events is recorded. For the non-equilibrium MCM rate determination, the number of collisions and high energy fraction are accumulated. The actual TCE rate coefficient, collision rate and high energy fraction are computed from:

$$k_f = \frac{N_{react}}{N_{pairs}} (\sigma g)_{max}, \quad Z_c = \frac{N_{collisions}}{N_{pairs}} (\sigma g)_{max}, \quad F = \frac{N_{energy}}{N_{collisions}} \quad [7]$$

In this study the dissociation reaction of molecular oxygen is considered. Results are presented for dissociation through $O_2 + O_2$ collisions. Similar results were found for dissociation through $O_2 + O$ collisions. Species specific collision cross-section data of Gupta *et al.*¹¹ have been used to fit the following power law viscosity relations at a reference temperature $T_{ref} = 1000K$:

$$O_2 + O_2: \quad \mu_r = 4.91 \cdot 10^{-5} \text{ kg/m/s}, \quad \nu = 0.19$$

$$O_2 + O: \quad \mu_r = 4.50 \cdot 10^{-5} \text{ kg/m/s}, \quad \nu = 0.25$$

$$O + O: \quad \mu_r = 4.70 \cdot 10^{-5} \text{ kg/m/s}, \quad \nu = 0.28$$

The reaction rate data of Park¹² have been used for the equilibrium reaction rate:

$$O_2 + O_2: \quad k_f^* = 2.288 \cdot 10^{-16} (T / \theta_D)^{-1.5} \exp(-\theta_D / T) \text{ m}^3 / \text{s}$$

$$O_2 + O: \quad k_f^* = 1.144 \cdot 10^{-15} (T / \theta_D)^{-1.5} \exp(-\theta_D / T) \text{ m}^3 / \text{s}$$

Where $\theta_D = 59500K$ is the dissociation temperature of oxygen. The characteristic vibrational temperature of oxygen for the harmonic oscillator model was taken as 2256K.

The overall temperature and the fraction of the total energy in the translational mode were varied between 5000-20000K and 0.2-1.0 respectively. The temperatures of the rotational and vibrational modes were equal. These cases covered the range corresponding to the flow which may be found behind a shock wave where the translational temperature is above that of the rotational and vibrational temperatures, or in an expansion where the internal modes may be frozen at a temperature above that of the translational temperature. Separate adjustment of the components of translational temperature for a given total translation energy was found to have negligible influence and is not included here. The sampling continued until at least 10^3 reactions and at least 10^6 collisions had been computed for each condition.

In the TCE model, the probability of a reacting collision is a function of the total collision energy of the colliding particles. However, the probability function also includes a term corresponding to the average number of internal degrees of freedom. Since vibration is rarely fully excited, it might be expected that the number of vibrational degrees of freedom in the TCE probability function should also vary. However, according to Haas¹⁴, the variation of the average number of internal degrees of freedom over the chemically reacting region of a general flow-field is small and thus may be taken approximately as a constant value characteristic of the overall flow-field. In this study, the overall temperature has been used to define the constant number of vibrational degrees of freedom in the TCE model.

The expression for the fraction of high-energy collisions F^* in equation [5], which is used in the rate equation [4] corresponds to the continuously distributed harmonic oscillator model for the vibrational energy levels. However, the quantized version of the vibrational energy distribution was used in the collision calculations, since this is generally considered more accurate¹⁵. Thus the reaction rate given by equation [4] differs slightly from the equilibrium rate, even for equilibrium conditions. As noted by Gimelshein *et al.*¹⁵, the TCE chemistry model is also derived for continuously distributed vibrational levels and a similar small difference between the theoretical equilibrium rate and the actual TCE rate at equilibrium is expected.

The left plot in Fig. 1 shows the overall reaction rates as computed by the TCE method and rate corrected MCM. The overall temperature is 20000K and the translational and vibrational temperatures vary between 10000-30000K and 0-10000K respectively to give a range of non-equilibrium conditions, as expressed by the fraction of the total energy in the translational modes. The right plot in Fig. 1 shows how the collision rate and high energy fraction vary for these different conditions.

It can be seen that when the majority of the energy is in the translational modes, the reaction rate decreases significantly. This is because all of the internal energy contributes to the reaction whilst only the relative components of the translational energy contribute. The reaction rate decreases faster as the fraction of energy in the translational mode approaches unity. Since it is the overall temperature which is constant rather than the total energy, the overall energy (and hence the rate) decreases due to the reducing number of vibrational degrees of freedom. A reduced collision rate causes the reaction rate to decrease when the majority of the energy is in the internal modes.

The rate corrected method closely matches the TCE model. The small variation present is due to the variation of the distribution of high energy particles between the non-equilibrium and nearby equilibrium condition.

These tests of the rate correction are not particularly severe since we have assumed that equilibrium distributions exist in each mode. However, they do demonstrate that a simple correction can be used to account for the actual number of collision pairs with sufficient energy to react.

B. FLOW SIMULATION

To test the non-equilibrium rate equation [4] further, we require a flow-field where significant chemical reactions occur in regions of thermal non-equilibrium. To this end, we consider a flat plate aligned perpendicularly to a high Mach number rarefied flow of diatomic oxygen. A two-dimensional simulation domain is used so that the plate is infinitely wide. The free-stream conditions and computational parameters are given in Table 1. Although the density is very low, the stagnation temperature behind the shock is of the order of the dissociation temperature of oxygen. As a result, although the collision rate is low, the fraction of potential reacting collisions is high.

The vertical plate has a height of approximately 1 nominal upstream mean free path. Here the nominal mean free path is defined as:

$$\lambda_{nom} = 2\mu_{\infty} / \left(\rho_{\infty} \sqrt{8kT_{\infty} / \pi m} \right)$$

The plate is modelled as a diffuse reflector with complete accommodation in the normal and translational components of thermal energy and the rotational energy. The vibrational accommodation coefficient is zero and no surface chemical reactions are modelled. The downstream boundary is modelled as a vacuum boundary; the normal component of Mach number is supersonic everywhere along this boundary. Particles entering the domain through the top boundary have properties characteristic of the free-stream. This is expected to introduce a small error due to the slightly higher temperatures along this boundary. A simulation was run with the top boundary location twice as far from the plate and the resulting flow-field differences were negligible.

The collision rate data given in the previous section is used with the VHS collision model. The serial application⁶ of the Borgnakke-Larsen (BL) energy exchange model is implemented with constant rotational and vibrational exchange probabilities of 0.2 and 0.02 respectively. The continuously distributed model of rotational energy and the discrete unbound harmonic oscillator model of vibrational energy are used.

The flow-field is sampled at intervals of $5 \Delta t$ with the samples taken before and after the collision routine alternately as suggested by Rebrov and Skovorodko¹⁶. The macroscopic parameters are calculated at intervals of $20 \Delta t$ with the sample reset at these intervals during the approach to steady state. Steady state is assumed to have occurred at a non-dimensional time of 5 corresponding to the free-stream flow traversing the computational domain five times. The sampling is continued until a non-dimensional time of 20 is reached. The domain is divided into 4 regions for the purpose of calculating the cell-structure. The cell size in each direction is varied using geometric progressions to concentrate cells near the plate.

The macroscopic chemistry method is implemented according to Lilley⁸ where particles are selected at random for reaction and the dissociation energy is removed from the translational mode only. Chemical reactions are considered at each time-step using the modified Arrhenius rate data given in the previous section and the overall cell temperature. Reverse reactions were included in an initial simulation using the equilibrium constant data of Prabhu and Erickson¹⁷. Since no recombination events were found to occur, recombination reactions were subsequently excluded in all cases. For case 4, the rate correction

is implemented using the method described above assuming continuously distributed internal modes. The TCE method is implemented in the collision routine before the serial BL procedure. The proportional energy exchange method¹⁴ is used for consistency with the MCM energy exchange method. The number of vibrational degrees of freedom in the TCE probability function is set as a constant value characteristic of a flow-field at a temperature of 5000K. Only 0.2% of the total CPU time was devoted to computing the reaction rate correction.

Simulations using the TCE, MCM and new rate corrected MCM (NEQ-MCM) chemistry models have been run for the free-stream conditions list in Table 1. Contours of the atomic oxygen mole fraction and translational temperature for the TCE and MCM methods are shown in Fig. 2. The TCE model has resulted in more dissociation with the chemically reacting region extending further out from the plate. Contours of the translational temperature show that the shock is marginally thicker in the TCE case and that the translational temperatures in the wake region behind the plate are similar. The translational, rotational and vibrational temperatures and the atomic oxygen mole fraction along the stagnation streamline are shown in Figs. 3 and 4. Although the flow-fields are qualitatively similar, some quantitative differences are present. In the MCM case, the peak translational temperature within the shock is approximately $5T_\infty$ lower, and behind the plate approximately $5T_\infty$ higher than the TCE result. The rotational and vibrational temperatures are significantly lower in the TCE case. The MCM simulation predicts between 5 and 10% less dissociation in the region behind the plate and almost 15% less dissociation in the region directly in front of the plate.

Properties along the stagnation streamline for the rate corrected MCM simulation are shown in Figs. 3 and 4. The rate correction has reduced the differences between the MCM and TCE solutions. The peak translational temperatures in the shock for the two methods agree and the difference between the local maximums of the translational temperature behind the plate has been reduced. The non-equilibrium reaction rate has led to a generally increased dissociation rate in front of and behind the plate. There is a marked difference between the rotational and vibrational temperatures for TCE and MCM, for both forms of reaction rate.

Coefficients of drag, shear and heat transfer are shown for each case in Table 2. The variation of the total drag and shear forces on the plate is negligible over all the cases, including the non-reacting flow-field. However the heat transfer coefficient does vary considerably. Less heat transfer occurs for reacting flow-fields since energy has been absorbed in the dissociation processes within and behind the shock. The MCM predicts a heat transfer coefficient 21% higher than the TCE method while the NEQ-MCM predicts the same heat transfer coefficient as the TCE case.

The overall fraction of reacting collisions per particle for the TCE, MCM and NEQ-MCM cases are shown in Fig. 5. Within the shock, up to 24% (TCE), 20% (NEQMCM) and 12% (MCM) of the collisions are reacting. In the region behind the plate where the densities and hence the collision rates are much lower, less than 4% of the collisions result in a reaction for the TCE and NEQ-MCM cases. For the MCM case, proportionally more reactive collisions occur further downstream. In the uncorrected MCM, reactions are less likely to occur until some energy has been transferred to the rotational and vibrational modes.

V. DISCUSSION

It is useful to consider again how we estimate the non-equilibrium reaction rate in the MCM simulations. To calculate the required number of reaction events, we have used the actual collision rate and the actual number of particles with sufficient energy to react, as found in the simulations. We have assumed, in effect, a steric factor equal to the steric factor at equilibrium, as determined by the specified equilibrium reaction rates. The equilibrium steric factor incorporates information regarding the orientation of particles, their relative vibrational frequencies and phases, the amount of total energy they have above the threshold energy and other unknown factors. We have not specified how the energy is distributed amongst the product particles or which particles we will choose for the reaction (the distribution of reactant particles).

In the flow-field simulation considered, the fraction of reacting collisions was not small and the predicted heat transfer coefficient from the modified and unmodified macroscopic chemistry methods varied significantly. Thus for this simulation, the use of equilibrium reaction rates in the MCM resulted in some probable inaccuracies. The simple rate correction produced results closer to the TCE method with the predicted heat transfer to the plate being exactly the same. The discrepancies between the rotational and vibrational temperatures may be attributed to the mechanics of accounting for the dissociation energy in the MCM method, rather than the reaction rate specifically. In the MCM method, the dissociation energy was removed from the translational mode only, whereas in the TCE method, energy may be removed from all modes. It is expected that this may have led to the higher than expected internal temperatures in the MCM simulation cases. The MCM is not restricted to the specific energy disposal methods used in this study.

The simulation considered here has both a very high speed flow where the kinetic energy is on the order of the dissociation energy and a set of reaction rates which are fast in comparison to other available experimental data¹¹. The reaction rate data used in this study is based on the two-temperature model of Park¹². Park states that the model is applicable up to translational temperatures of 50000K, but only to a geometric temperature of 10000K. In this study, the overall cell temperature was used when evaluating the reaction rate. Thus, the dissociation rates observed in this study were above those which are recommended by Park for these conditions. Lilley and Macrossan⁹ have considered a similar flow-field and made comparisons between the macroscopic and total collision energy methods for the flow of oxygen over a blunt-ended cylinder at Mach 45. In that study, the slower reaction rate data of Gupta *et al.*¹¹ was used. The resulting differences between the translational and rotational temperatures and the mole fraction of atomic oxygen along the stagnation streamline between the MCM and TCE predictions were negligible. A small difference in vibrational temperature was noted which may be due to the method of energy disposal previously discussed. It is thus apparent that the use of a very fast reaction rate in the current study is the reason for the significant departure of the reaction rate from the equilibrium rate.

VI. CONCLUSIONS

The advantages of the macroscopic chemistry method are its flexibility and generality. It would be possible, for example, to use detailed vibrational state dependent reaction rates and an-harmonic oscillator vibrational levels. In previous work with MCM the reaction rate in any cell was taken as the equilibrium reaction rate, regardless of the degree of non-equilibrium in the flow. This worked well because reacting collisions were rare events and thermal equilibrium was established before any significant number of reaction events took place. It was not known how the method would perform if a significant number of reaction events took place in conditions of non-equilibrium. We have addressed

that issue here by assuming reactions rates for oxygen dissociation much greater than those recommended in the literature.

We have demonstrated a simple procedure for calculating the reaction rate in the macroscopic chemistry method in conditions of strong non-equilibrium. The procedure takes into account the non-equilibrium collision rate and the fraction of high-energy collision pairs which arise from the energy distribution in the cell and the collision cross-section (collision probability) used in the DSMC collision procedure. This same information is captured by the standard TCE method. The MCM is more general in that it is not tied to the VHS collision cross-section; it could be used with a cross-section for a more realistic inter-molecular potential which includes attractive as well as repulsive forces. It is plausible that the non-equilibrium high-energy collision rate arising from such a realistic potential should be reflected in the chemical reaction rate.

The remaining factor which determines the collision rate is the steric factor, the fraction of sufficiently energetic collisions which result in a reaction event. In MCM we assume, in effect, that the steric factor is the same for equilibrium conditions as for non-equilibrium conditions. In TCE a reaction probability as a function of collision energy is specified and adjusted so that, when averaged over all high-energy collisions at equilibrium, it yields the equilibrium steric factor. In both methods we know the equilibrium steric factor from the specified equilibrium reaction rate. In the TCE method the average of the reaction probability for non-equilibrium conditions, the effective steric factor, varies from its equilibrium value, which is why the MCM reaction rate differs slightly from the TCE rate in non-equilibrium conditions. Considering the scarcity of experimental data, it is difficult to say whether the particular variation of the steric factor arising from the TCE model is more realistic than the MCM approximation. We regard the Macroscopic Chemistry Method, with the reaction rate determined by equation [4], as a reasonable approach to modelling chemical reactions in the DSMC method in both near equilibrium and non-equilibrium flows.

REFERENCES

1. Boyd, I., "Nonequilibrium chemistry modelling in rarefied hypersonic flows," in *Chemical Dynamics in Extreme Environments*, edited by R. A Dressler, World Scientific, Singapore, 2001, pp. 81-137.
2. Bose, D. and Candler, G., "Kinetics of the $N_2+O \rightarrow NO+N$ reaction under thermodynamic nonequilibrium," *J. Thermodynamics and Heat Transfer*, Vol. 10, No. 1, 1996, pp. 148-154.
3. Boyd, I., Bose, D. and Candler, G., "Monte carlo modelling of nitric oxide formation based on quasi-classical trajectory calculations," *Physics of Fluids*, Vol. 9, No. 4, 1996, pp.1162-1170.
4. Wysong, I., Boyd, I., "Direct Simulation Monte Carlo dissociation model evaluation: comparison to measured cross sections," *J. Thermodynamics and Heat Transfer*, Vol. 16, No. 1, 2002, pp.83-93.
5. Wadsworth, W. and Wysong, I., "Vibrational favouring effect in DSMC dissociation models," *Physics of Fluids*, Vol. 9, No. 12, 1997, pp.3873-3844.
6. Bird, G.A, *Molecular gas dynamics and the direct simulation of gas flows*, Clarendon Press, Oxford, 1994.
7. Lilley, C. R. and Macrossan, M. N. "A macroscopic chemistry method for the direct simulation of gas flows," *Physics of Fluids A*, Vol. 16, No. 6, 2004, pp. 2054-2066.
8. Lilley, C.R, "A macroscopic chemistry method for the direct simulation of non-equilibrium gas flows", PhD thesis, The University of Queensland, 2005.

9. Lilley, C.R and Macrossan, M.N., "Applying the Macroscopic Chemistry Method to Dissociating Oxygen", *25th International Symposium on Rarefied Gas Dynamics*, 21-28 July, 2006, St. Petersburg, Russia, Proceedings, ed. M. S. Ivanov and A. K. Rebrov (Siberian Branch of the Russian Academy of Sciences, 2007), pp. 367-372.
10. Lilley, C.R. and Macrossan, M.N., "Modeling Vibrational-Dissociation Coupling with the Macroscopic Chemistry Method," In *24th International Symposium on Rarefied Gas Dynamics*, 10-16 July, 2004. AIP Conference Proceedings, Vol. 762 (Ed Capetilli, M) pp. 1019-1024.
11. Gupta, R., Yos. J., Thompson, R. and Lee, K. *A review of reaction rates and thermodynamic and transport properties for an 11-species air model for chemical and thermal nonequilibrium calculations to 30000K*, NASA, Washington, 1990, NASA reference publication 1232.
12. Park, C., *Nonequilibrium Hypersonic Aerothermodynamics*, Wiley, New York, 1990.
13. Vincenti, W. and Kruger, C., *Introduction to physical gas dynamics*, Wiley, New York, 1975.
14. Haas, B., "Models of energy exchange mechanics applicable to a particle simulation of reactive flow," *J. Thermodynamics and Heat Transfer*, Vol. 6, No. 2, 1992, pp.478-489.
15. Gimelshein, S., Gimelshein, N. Levin, D., Ivanov, M. and Wysong, I., "On the use of chemical reaction rates with discrete internal energies in the direct simulation Monte Carlo method," *Physics of Fluids*, Vol. 16, No. 7, pp. 2442-2451.
16. A. K. Rebrov and P. A. Skovorodko, "An Improved Sampling Procedure in DSMC Method", Proceedings of the 20th International Symposium on Rarefied Gas Dynamics (ed. Ching Shen), Peking University Press, Beijing, China, 1997, pp. 215 - 220.
17. Prabhu, R. and Erickson, W., "A rapid method for the computation of equilibrium chemical composition of air to 15000K", NASA, Washington, 1988, NASA reference publication 2792.

TABLES

Free-stream conditions:	Computational parameters	Cases
$M_\infty : 30$ $T_\infty : 300K$ $\rho_\infty : 10^{-6} kg / m^3$ $\lambda_{nom} : 0.096m$ $X_{O_2} : 1$	$Plate\ height : 0.1m$ $Cells : 25200$ $Simulators : 10^6$ $Sample\ size : 3 \times 10^9$ $\Delta t = 5 \times 10^{-7} s$	1: Non-reacting 2: ‘Standard’ TCE 3: Standard MCM 4: Corrected MCM
Boundary conditions:	Simulation details	
$Diffuse\ reflection$ $T_w = 300K$ $a_n = a_{tan} = a_r = 1.0\ a_v = 0.0$	$\phi_r = 0.2$ $\phi_v = 0.02$	

Table 1 Simulation details

Case	C_D	C_S	C_H	C_H normalized
Non-reacting	1.949	0.116	0.610	1.32
TCE	1.957	0.119	0.463	1
MCM	1.953	0.117	0.558	1.21
NEQ-MCM	1.931	0.118	0.465	1.00

Table 2 Plate force and heat transfer coefficients

FIGURES

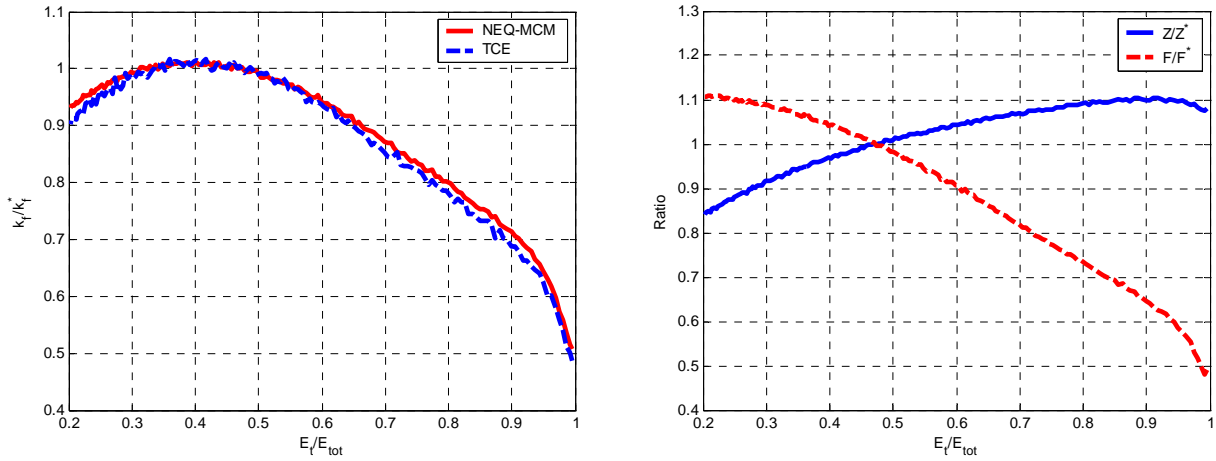


Figure 1 Non-equilibrium rate comparisons at $T_{ov} = 20000K$. Ratio of equilibrium to non-equilibrium rate (left) for MCM and TCE. The MCM rate correction accounts for the non-equilibrium high energy fraction and non-equilibrium collision rates shown in the right figure. Equilibrium conditions correspond to $E_i / E_{tot} \approx 0.474$.

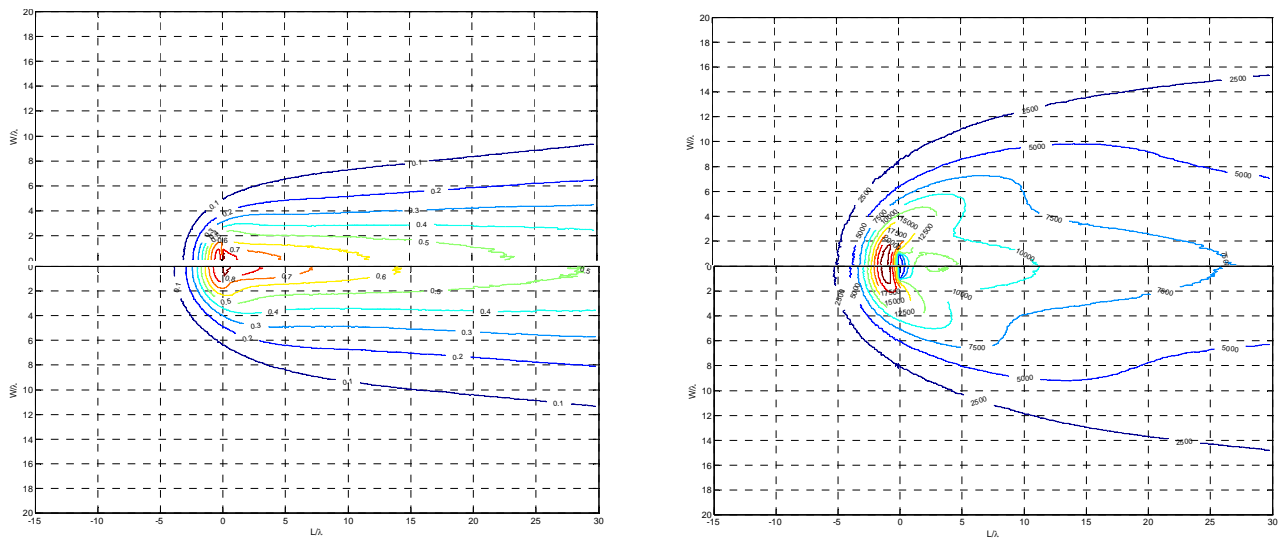


Figure 2 Contours of mole fraction of atomic oxygen (left) and translational temperature (right) from MCM with $k_f = k_f^*$ (top) and TCE (bottom) simulations.

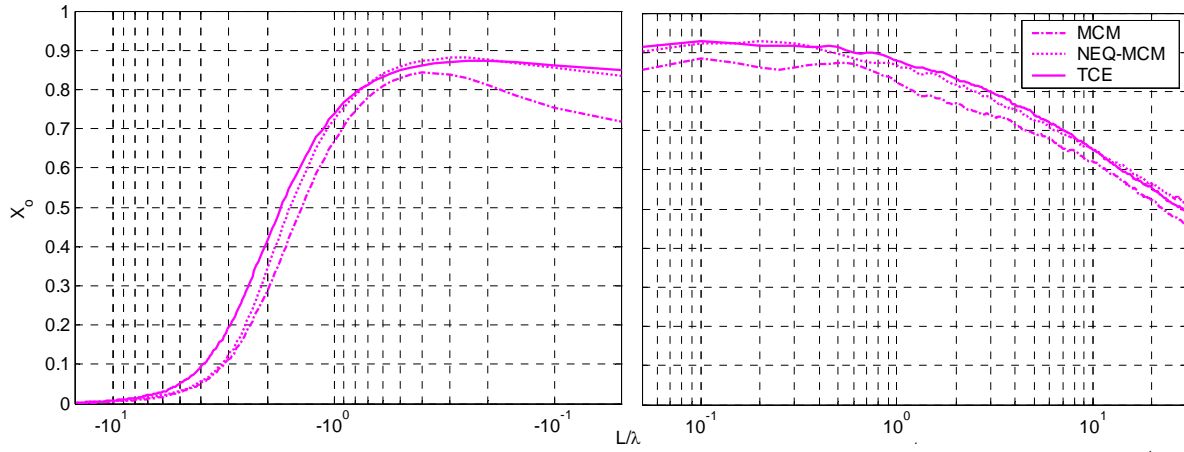


Figure 3 Mole fraction of atomic oxygen along the stagnation streamline for MCM ($k_f = k_f^*$), NEQ-MCM (k_f from [4]) and TCE cases. A logarithmic scale is used. The left and right plots correspond to the regions left and right of the plate respectively.

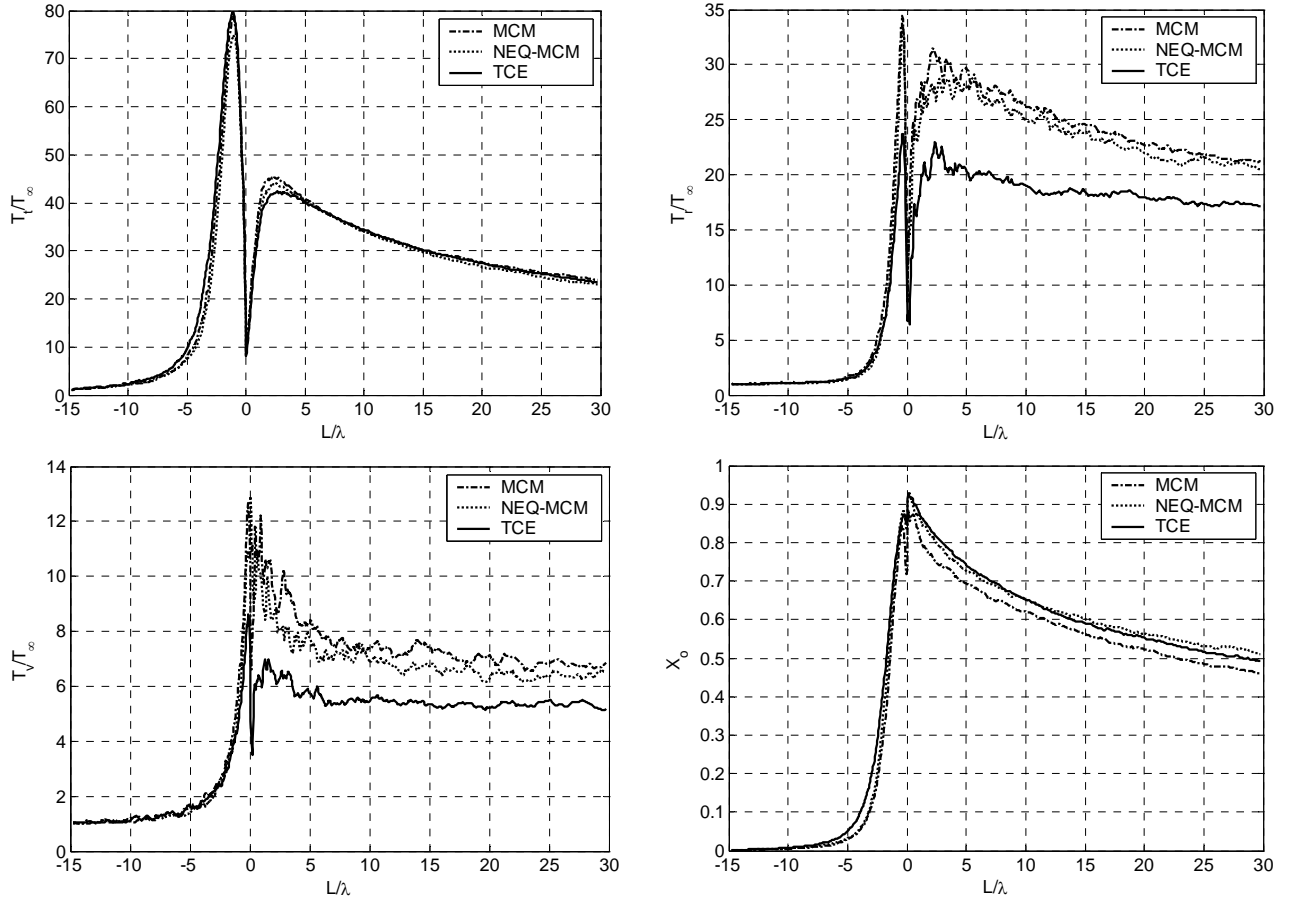


Figure 4 Properties along the stagnation streamline. translational temperature, rotational temperature, vibrational temperature and mole fraction of atomic oxygen.

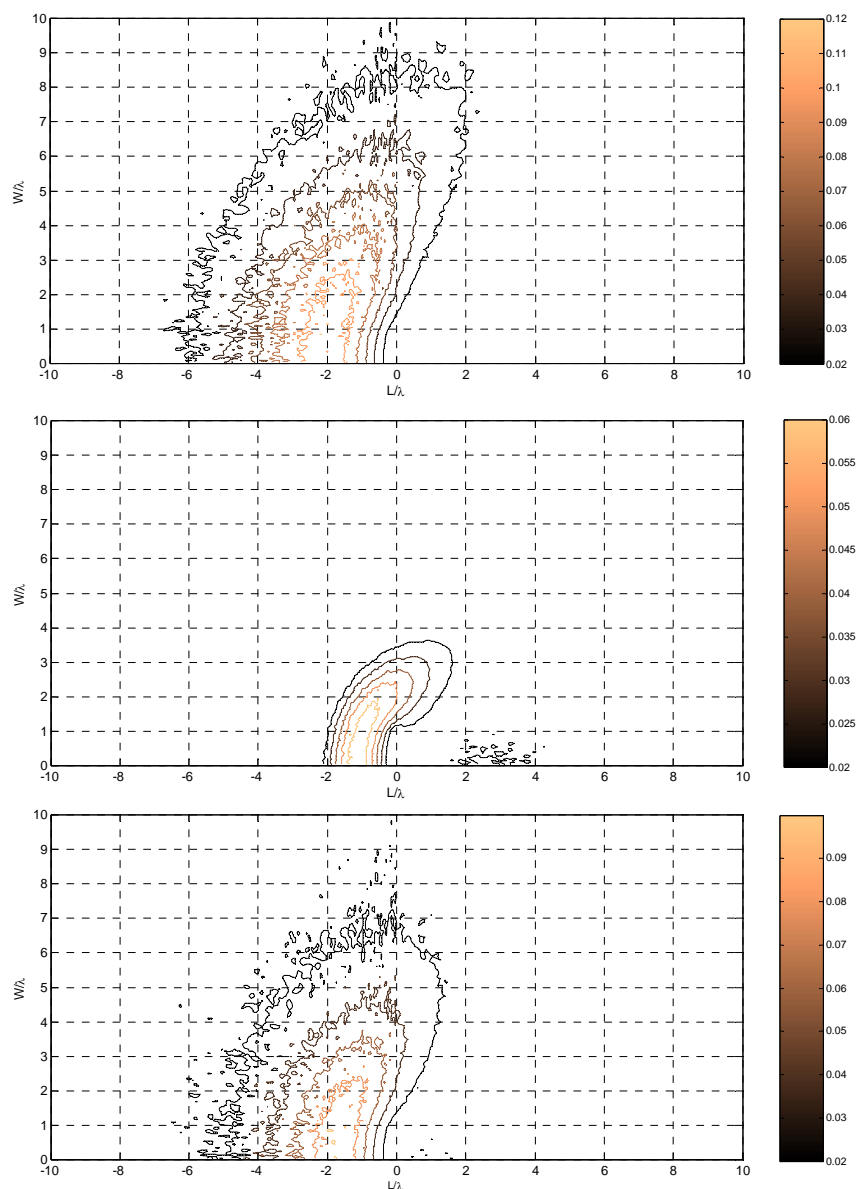


Figure 5 Fraction of reacting collisions per particle for TCE (top), MCM (middle) and NEQ-MCM (bottom) cases. The TCE and NEQ-MCM solutions show similar characteristics. The MCM solution shows a reaction incubation period where the internal temperatures increase such that the overall temperature is sufficiently high for reactions to take place.